Inhalation Toxicology, 14:705–720, 2002

0895–8378/02 $12.00 + .00
DOI: 10.1080/0895837029008459 3

Taylor&Francis
healthsciences

COMPUTER SIMULATIONS OF PARTICLE DEPOSITION IN THE LUNGS OF CHRONIC OBSTRUCTIVE PULMONARY DISEASE PATIENTS

R. A. Segal

U.S. Environmental Protection Agency, Experimental Toxicology Division, National Health and Environmental Effects Research Laboratory, Research Triangle Park, North Carolina, and North Carolina State University, Raleigh, North Carolina, USA

T. B. Martonen

U.S. Environmental Protection Agency, Experimental Toxicology Division, National Health and Environmental Effects Research Laboratory, Research Triangle Park, North Carolina, USA

C. S. Kim

U.S. Environmental Protection Agency, Human Studies Division, National Health and Environmental Effects Research Laboratory, Chapel Hill, North Carolina, USA

M. Shearer

North Carolina State University, Raleigh, North Carolina, USA

Epidemiology data show that mortality rates for chronic obstructive pulmonary disease (COPD) patients increase with an increase in concentration of ambient particulate matter (PM). This is not seen for normal subjects. Therefore, the U.S. Environmental Protection Agency (EPA) has identified COPD patients as a susceptible subpopulation to be considered in regulatory standards. In the present study, a computer model was used to calculate deposition fractions of PM within the lungs of COPD patients. The morphology of COPD lungs was characterized by two distinct components: obstruction of airways (chronic bronchitis component), and degeneration of alveolar structure (emphysema component). The chronic bronchitis component was modeled by reducing airway diameters using airway resistance measurements in vivo, and the emphysema component was

Received 22 August 2001; sent for revision 11 October 2001; revision received 4 January 2002; accepted 14 January 2002.

R. A. Segal was funded by the NCSU/EPA Cooperative Training Program in Environmental Sciences Research, training agreement CT826512010.

The information in this document has been funded wholly (or in part) by the U.S. Environmental Protection Agency. It has been subjected to review by the National Health and Environmental Effects Research Laboratory and approved for publication. Approval does not signify that the contents reflect the views of the agency, nor does mention of trade names or commercial products constitute endorsement or recommendation for use.

Address correspondence to Ted Martonen, U.S. EPA, ETD, NHEERL, Mail Drop 74, RTP, NC 27711, USA. E-mail: martonen.ted@epa.gov

modeled by increasing alveolar volumes. Calculated results were compared with experimental data obtained from COPD patients for controlled breathing trials (tidal volume of 500 ml, respiratory time of 1 s) with a particle size of 1 μm. The model successfully depicts PM deposition patterns and their dependence on the severity of disease. The findings indicate that airway obstructions are the main cause for increased deposition in the COPD lung.

An increase in mortality and morbidity for patients with cardiovascular or chronic obstructive pulmonary disease (COPD) has shown a close association with concentrations of airborne particulate matter (PM) (Seaton et al., 1995; Schwartz, 1996; Wordley et al., 1997). Mechanisms by which such adverse health effects occur are not known. However, a marked enhancement in deposition dose in the patients with lung disease could be a contributing factor for the observed effects.

Experimental studies have shown that total lung deposition of inhaled particles is much greater in patients with obstructive airway disease such as asthma and COPD compared to healthy individuals (Kim, 1989; Kim & Kang, 1997). The deposition enhancement in the patient is generally confined to the central airway regions, indicating a critical role of obstructed airways in deposition enhancement. Although airway obstructions take place in many different forms in COPD (even and uneven narrowing, focal constriction, excessive mucus, etc.), experimental studies have consistently demonstrated enhanced aerosol deposition in both animal models in vivo (Kim, 1989; Kim et al., 1989) and specific in vitro airway models (Kim et al., 1983; Kim & Eldridge, 1985) regardless of the types of obstruction used.

There have been previous modeling efforts to examine deposition of particles in healthy lungs (Kuempel et al., 2001; Lazaridis et al., 2001; Smith et al., 2001). Studies on deposition in diseased lungs have also been performed (Anderson et al., 1989; Laube et al., 1986; Svartengren et al., 1990). However, the literature is scarce with regard to modeling efforts for diseased lungs.

In this article, we describe a computer model developed to understand how particle deposition in COPD lungs differs from deposition in healthy lungs. Computer models have the potential to save considerable time and expense when compared to studies relying solely on human subject testing. Moreover, the data from the computer model is much more extensive (i.e., different factors and more variables can be studied) and detailed (e.g., localized doses delivered to target sites can be calculated) than the data from human subject experiments. Our deposition code has previously been validated by comparing simulation results to human subject data from various laboratories. (Martonen, 1983; Martonen & Katz, 1993a, 1993b, 1994; Segal et al., 2000). In those comparisons, restricted to healthy subjects, the effects of ventilation, particle characteristics, and lung size were investigated.

The goal in this effort was to isolate the effects of morphology changes. While there are many diseases that affect airway morphology, we focused on COPD as a representative airway disease. Among the many symptoms

and disease processes associated with COPD, (NLHEP, 1998; Rennard, 1998) we chose to simulate two major components, namely chronic bronchitis and emphysema. Emphysema usually develops in the late phase of COPD and becomes an integral part of severe COPD.

Symptoms of chronic bronchitis include increased mucus production and chronic coughing. Coughing causes irritation to airway walls and encourages the production of collagenous connective tissue. The combination of increased mucus, excess tissue, and inflammation leads to a reduction of airspace within the tracheobronchial tree. The reduction is less pronounced in the large airways because morphological structures (such as muscle tone and cartilaginous rings) keep these airways more rigid.

Emphysema is characterized by a deterioration of the alveolar walls. The breakdown of alveolar structure allows the alveolar region to expand, causing the volume to increase. The erosion of structure also induces a decrease in interluminal pressure and a consequent reduction in the patient's ability to exhale.

METHODS

The purpose of this work was to gain a better understanding of factors affecting PM deposition in the lungs of COPD patients. To do this, we developed a computer model, tested it against human subject data, and then used it to isolate distinct aspects of the disease. A detailed explanation follows as to how an existing computer model was modified to be used for this project, how the information from the clinical experiments was translated into input parameters for the computer program, and how the code was used to gain insight into the particle deposition patterns associated with COPD.

To test the model, we compared results of the simulations with human subject test data (Kim & Kang, 1997). The study measured deposition in COPD patients as compared with healthy subjects. In our simulations of the Kim and Kang (1997) human exposures we used total airway resistance (Raw) values measured for each subject, and a second set of measurements, the functional residual capacity (FRC) values. The FRC data were used to scale the total lung volume for each individual lung model after making adjustments for emphysema.

Theory

We begin with the definition of the model. We have taken our existing model for particle deposition in the lung (Martonen, 1982), which uses a standard lung morphology, and modified that morphology description to include the physical changes that result from COPD. The standard model was based on a healthy lung with a total volume of 4800 ml according to Weibel (1963). The Weibel lung model defines the human lung by 24 serial generations starting with the trachea as generation 0. The lung model modi-

fications depend on three parameters: percent alveolar degeneration, FRC, and Raw. The amount of alveolar degeneration is estimated by a range of percentages because the exact value for each patient is not known. The other two values (FRC, Raw) are measured for each test subject. Using these parameters we constructed a custom-made lung model for each test subject.

Starting from the standard (i.e., default) lung morphology, we implemented several different geometric scalings. In modeling the emphysema component of COPD, we capture the main effect of the above disease processes by increasing the alveolar volume. This is achieved by scaling the diameters of the alveolated airways; in the absence of systematic clinical data, various alveolar scaling factors were used. Alveolar volumes were increased by 10% to 30% to describe degeneration of the alveolar sac walls. The fraction of surface alveolated remained unchanged. Within this range, we found (see Results) that scaling the alveolar volumes did not affect the deposition patterns too significantly; therefore, a value of 30% was adopted for use. This modification increases the size of the alveolar region as compared to the total lung volume, a property preserved in subsequent morphology modification. In the present study we develop a computer model for particle deposition in lungs with obstructive airway disease with and without an emphysema component.

Next, using the FRC measurement, we scaled the airway diameters to adjust total lung volume. The FRC is the amount of air remaining in the lung after the subject exhales. The sum of the FRC with one half of the tidal volume determined the average lung size during a breathing cycle. The subjects we modeled had FRC values ranging from 1850 ml to 6820 ml, whereas our standard model was based on a healthy lung with a total volume of 4800 ml (Weibel, 1963). To accommodate this variation, all of the airway diameters (hence the airway volumes) were modified by a uniform FRC scaling factor. The FRC scaling factor is greater than 1 if the subject's lung was larger than the original Weibel lung and less than 1 if the subject's lung was smaller than the Weibel lung. This scaling does not negate the previous scaling for emphysema. The emphysema scaling increased the size of the alveolar region relative to the remaining lung. That relative increase is not lost by resizing the entire lung to adjust for individual FRC measurements. The use of a uniform FRC scaling factor for the diameters is based on the research of Hughes et al. (1972) who determined that airway diameters scale proportionally to the cube root of the lung volume while the lengths of the airways are relatively unchanged. Although the work of Hughes et al. was performed using excised lungs and this could have affected the conclusions, it provides a reasonable starting point for applying scaling to the model.

Finally, we accounted for increased airway resistance in the COPD lung by using the measured Raw value for each subject. The Raw value, an indicator of total airway resistance, increased due to the chronic bronchitis

component of COPD and was used to determine the diameter reduction in generations 0–16 (i.e., conduction airways). Since the flow resistance is significantly larger in generations 0–16, changing the diameters in this region will provide enough impact to increase the Raw of the standard lung (0.21 cm H_2O•s/L) to equal that of a patient with COPD. Therefore, we modeled the airspace reduction by narrowing all airways with a particular generation uniformly, but did allow for variations between different generations. The airway resistance (Raw) value, which was measured for each human subject in the clinical trials, determined the extent of airway narrowing.

Note that measured Raw has two components, flow resistance in the upper airways (R_{uaw}) and that in the lower airways (R_{law}). R_{uaw} is the resistance in the oropharynx and the larynx and R_{law} is the resistance in the tracheobronchial and pulmonary airways. Because the upper airways are not affected by the disease processes associated with COPD, R_{uaw} is unaffected by COPD. In fact, in this study we are examining deposition only in the lower airways and the effects of COPD therein. In a healthy subject, $R_{uaw} \approx R_{law} \approx$ ½Raw (Hyatt & Wilcox, 1961). In the studies of Kim and Kang (1997), Raw of normal subjects was 1.5. We assume that the COPD subjects have normal resistance in the upper airways. Therefore, 0.75 (= ½Raw) should be subtracted from Raw of COPD patients for the present modeling study because we are only modeling particle deposition in the lower airways.

As a first approximation of chronic bronchitis, a single bronchitis scaling factor was used for all the airways in generations 0–16. Because of morphological structures (e.g., cartilaginous rings), airways 0–7 (i.e., large airways) are less affected by the narrowing mechanisms of the chronic bronchitis. Therefore, a refinement to the model was to have greater diameter reduction in generations 8–16 (i.e., small airways) than in generations 0–7. As an initial estimate of the variation in reduction, we reduced the original bronchitis scaling factor by 10% in generations 0–7 and increased the bronchitis scaling factor in generations 8–16 to maintain the same Raw value.

Resistance

For completeness, we describe in more detail how the airway diameters are scaled based on the Raw measurement. Because the dimensions are the same for each airway in a given generation, the resistance is also the same. The equation for resistance, r_i, in one airway in generation i has been formulated by Pedley et al. (1970):

$$r_i = \frac{128 \cdot 1.85 \mu L_i}{4\pi d_i \sqrt{2}} \sqrt{\mathrm{Re}_i \frac{d_i}{L_i}} \tag{1}$$

where d_i is the airway diameter, L_i is the airway length, Re_i is the Reynolds number, and μ is the viscosity of air. As in the studies of Kim et al. (1983), we view airways of the same generation as resistors in parallel. Thus, total

resistance in generation i, R_i, is equal to $2^{-i}r_i$. The resistance of the entire airway structure is obtained by regarding the generations of the lung as resistors in series. Therefore, the total airway resistance is equal to the sum of the resistance in each generation. However, we only want to scale the diameters of the airways in the tracheobronchial region (TB). The diameters in the pulmonary region (P) will remain unaffected by the Raw adjustment. Hence, we may compute

$$R_{TB} = \sum_{i=0}^{16} R_i \qquad \text{and} \qquad R_P = \sum_{i=17}^{23} R_i \tag{2}$$

The scaling factor α is given by:

$$\alpha = [(R_{law} - R_P) / R_{TB}]^{1/4} \tag{3}$$

The two measured values, FRC and Raw, used to create the modified lung morphology for an individual patient are determined by conditions in distinct regions of the lung. FRC, which is a measurement of lung volume, is mostly accounted for in the pulmonary region (generations 17–23) and Raw, the total airway resistance, is a characterization of the tracheobronchial region (generations 0–16). That is, there is relatively little volume (~150 ml) in the tracheobronchial region and relatively little flow resistance in the pulmonary region. We use this to our advantage when designing a scaling algorithm. We can effectively change the diameters based on the Raw value without significantly affecting the previously achieved lung volume. Similarly, it is possible to scale the lung model based on the FRC after modifying the tracheobronchial region to reflect the proper Raw value without compromising the resistance value.

Next is a summary of the various scalings just described to account for the changes in lung morphology associated with COPD. We chose to scale based on the FRC value first. The scaling algorithm is listed next.

Scaling Algorithm

1. Scale the alveolar volumes to account for emphysema (i.e., increase total alveolar volume by 10–30%). Use alveolar scaling factor.
2. Scale the diameters of airways in each generation uniformly to achieve desired lung volume (equal to FRC + ½ tidal volume). Use FRC scaling factor.
3. Compute current total airway resistance, Raw.
4. Compute bronchitis scaling factor α for uniform constriction of airways in generations 0–16 to achieve desired Raw value.
5. Reduce bronchitis scaling factor for generations 0–7 by 10% and recalculate bronchitis scaling factor for generations 8–16 to maintain desired Raw value.
6. Calculate resulting volume in each generation for input into the computer code.

Experiment

The model was tested against human subject data from a clinical study, which we now briefly describe.

The experiments of Kim and Kang (1997) used monodisperse aerosols. The particles were 1 μm di-2-ethylhexyl sebacate oil aerosols generated with an evaporation–condensation aerosol generator. The test subjects were instructed to breath via the mouth in a controlled, predefined manner. The breathing conditions were defined by tidal volume of 500 ml and flow rate of 500 ml/s. FRC and Raw values were measured for each subject (see Table 1).

Some of the clinical parameters measured in the human subject experiments matched the standard input parameters (e.g., tidal volume) used in the computer code. However, in some cases it was necessary to take the measurements from the experiments (e.g., Raw) and translate the information into the values needed for the deposition code (e.g., airway diameters). This allowed us to customize the computer lung morphology to the characteristics of each patient. For discussion, we divide the parameters into four categories: breathing conditions, aerosol characteristics, simulation flags, and lung morphologies.

Breathing conditions Ventilation parameters were measured in the human subject experiments in terms of tidal volume (V_T) and flow rate (Q). In each set of experiments, the subjects were instructed to breath so that their inhalation and exhalation times were the same. From the measurements we computed inhalation (t_i) and exhalation (t_e) times to be $t_i = t_e = V_T/Q$. There was no pause time between inhalation and exhalation.

Aerosol characteristics Aerosol particles were defined in the experiments by two parameters: particle aerodynamic diameter (d_a) and material density (ρ). The particles used were nonhygroscopic and had aerodynamic diameters of 1 μm for the Kim (Kim & Kang, 1997) experiments. The 1 μm particle had a density of 0.91 g/cm^3. The geometric diameter can be calculated by: $d_g = \rho^{-1/2} d_a$.

TABLE 1. Lung function measurements for COPD subjects in the experiments of Kim and Kang (1997)

Patient	FRC (ml)	Raw (cm $H_2O \cdot L^{-1} \cdot s$)
1	3200	3.1
2	5500	5.7
3	3100	2.4
4	3980	6.1
5	4000	4.2
6	4800	4.5
7	4000	2.5
8	3400	2.6
9	2100	2.3
10	6200	4.3

Note. FRC, functional residual capacity of the lung. Raw, total airway resistance.

Simulation flags The subjects in the experiments used mouth breathing. A subject's nose was clamped with a nose clip to avoid any nasal breathing. In the computer code, this sets the mouth breathing simulation flag. In addition, a flag must be set to define whether the flow is uniform or parabolic. This choice applies to all of the airways in the model. In Table 2, we list the length of tube needed to achieve fully developed parabolic flow (Martonen et al., 1995). Because the flow is often neither plug nor fully parabolic, we ran a set of simulations with each option. It should be noted that the values computed for Reynolds number and entrance length for fully developed flow are based on formulas for flow under ideal conditions: that is, flow in a straight, smooth-walled tube. In the case of the lung, the airways are bifurcating, often curved, and of variable diameter. Also, the airway dimensions used in the calculations are those of Weibel and have not been modified to account for COPD. Therefore, the values listed in the table should be viewed as initial estimates. This further influenced the decision to include results using both the plug and the parabolic flow profile.

TABLE 2. Comparison of length required for fully developed parabolic flow with actual airway length

Airway generation	Airway diameter (cm)	Reynolds number	Airway length (cm)	Fully developed flow length (cm)
0	1.8	2352	12	254
1	1.22	1732	4.76	127
2	0.83	1278	1.90	64
3	0.56	945	0.76	32
4	0.45	588	1.27	16
5	0.35	378	1.07	8
6	0.28	237	0.90	4
7	0.23	144	0.76	2
8	0.186	89	0.64	1
9	0.154	53	0.54	0.49
10	0.130	32	0.46	0.25
11	0.109	19	0.39	0.12
12	0.095	11	0.33	0.06
13	0.082	6.6	0.27	0.03
14	0.074	3.5	0.23	0.015
15	0.066	1.76	0.20	0.007
16	0.060	1.2	0.165	0.004
17	0.054	0.7	0.141	0.002
18	0.050	0.3	0.117	0.001
19	0.047	0.16	0.099	0.0004
20	0.045	0.09	0.083	0.0002
21	0.043	0.06	0.070	0.0001
22	0.041	0.03	0.059	0.00007
23	0.041	0.01	0.050	0.00003

Note. Values are for the unmodified Weibel morphology (Weibel, 1963) at the mean respiratory flow rate of 500 ml/s.

Lung morphologies One set of simulations was run using all of the above specifications, corresponding to steps 1–6 in the previously described scaling algorithm. Additional simulations were run to isolate the components of COPD: namely, chronic bronchitis and emphysema. Referring back to the scaling algorithm, the following different lung models were used for the simulations:

A. Scaling for total lung volume only: step 2, 6.
B. Scaling for total lung volume and uniform airway reduction: steps 2, 3, 4, 6.
C. Scaling for total lung volume and non-uniform airway reduction: steps 2, 3, 4, 5, 6.
D. Scaling for total lung volume and alveolar degeneration: steps 1, 2, 6.
E. Scaling for total lung volumes, alveolar degeneration, and nonuniform airway reduction: steps 1, 2, 3, 4, 5, 6.

Item A is used as a control case. Items B and C focus on the chronic bronchitis component of COPD, item D focuses on the emphysema component of COPD, and item E combines the effects of emphysema and chronic bronchitis.

RESULTS AND DISCUSSION

The results are divided into two parts. In the first part, we compare the results of simulations with experimental data. In the second part, we study the details of deposition for an individual lung model. The lung morphologies for the first set of results are defined by using the entire scaling algorithm, whereas the lung morphologies for the second set only use parts A, B, C, D or E of the algorithm as described at the end of Methods.

For each patient, we created a model lung using the measured data (FRC and Raw) for that subject. A simulation was then performed using the experimental parameters (e.g., V_T) associated with that case. The total deposition values obtained from these computer runs are presented in Figure 1 with the deposition data obtained from the human subject experiments.

In Figure 1 we compare modeling results with the data from the human subject experiments (Kim & Kang, 1997). Lung deposition was calculated under the conditions of both parabolic and plug flow profiles. The simulations systematically underestimated particle deposition under the parabolic flow condition. However, model results agreed very well with experimental data under the plug flow condition. The present obstruction model used narrowed airways whereas airway obstruction in COPD consists of many irregular obstruction patterns. Aerosol deposition is greater in the airways with irregular obstructions than in the airways with simple narrowing (Kim et al., 1983; Kim & Eldridge, 1985; Kim, 1989). For example, when excessive mucus is accumulated locally and undergoes oscillatory motions from inter-

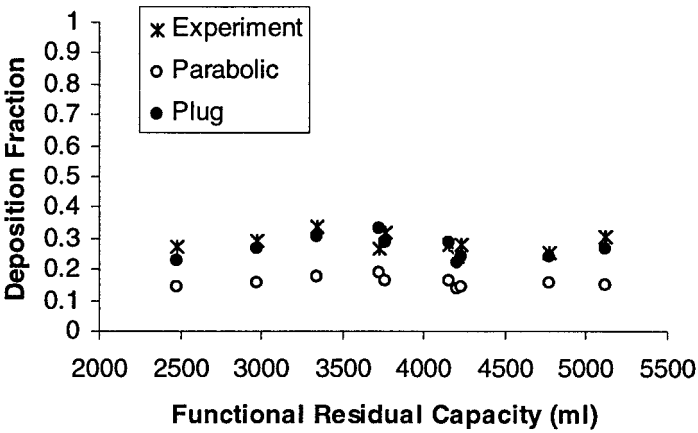

FIGURE 1. Comparison of computer simulations and human subject (COPD) data (Kim & Kang, 1997) for controlled breathing (V_T = 500 ml, Q = 500 ml/s) and particle size of 1 μm in aerodynamic diameter: ○ parabolic simulation, ● plug simulation, * experimental data.

action with airflow, aerosol deposition increases markedly with only a small increase in airway resistance (Kim & Eldridge, 1985). Under these situations airflow patterns would be quite irregular with some components of turbulence. Because the exact flow profiles for the airways in the lung are not known, analyzing the two extremes of possible profiles (plug and parabolic) allows for better approximation to the experimental data.

It should be noted that particle deposition values are higher for patients with COPD than in healthy subjects (Bennett et al., 1997; Kim & Kang, 1997). However, COPD involves a variety of disease processes which affect different regions of the lung and experimental data show an overall effect of morphological changes in COPD. The computer model allowed us to systematically investigate the individual components of COPD (chronic bronchitis and emphysema) and determine which had a greater impact on the experimentally observed deposition increase. However, one must notice that all of our morphological models use a symmetric and even distribution of airflow in the lung. Airflow distribution is very uneven in COPD. Therefore, our results should be viewed as a typical example applicable to conditions used in this study.

In Figures 2–7 we present results of simulations in which parameters have been adjusted to isolate the effects of individual components of COPD. To fix realistic values for parameters, we selected one individual from the Kim and Kang (1997) experiments and plotted more detailed results for that subject. We chose the subject with FRC = 3980 ml and Raw = 6.1. We selected this individual because of the high airway resistance measurement, surmising that it would be easier to notice effects of morphological changes if they are more pronounced.

In Figure 2, we plotted total deposition as a function of airway generation number. Each curve represents the deposition pattern resulting from a

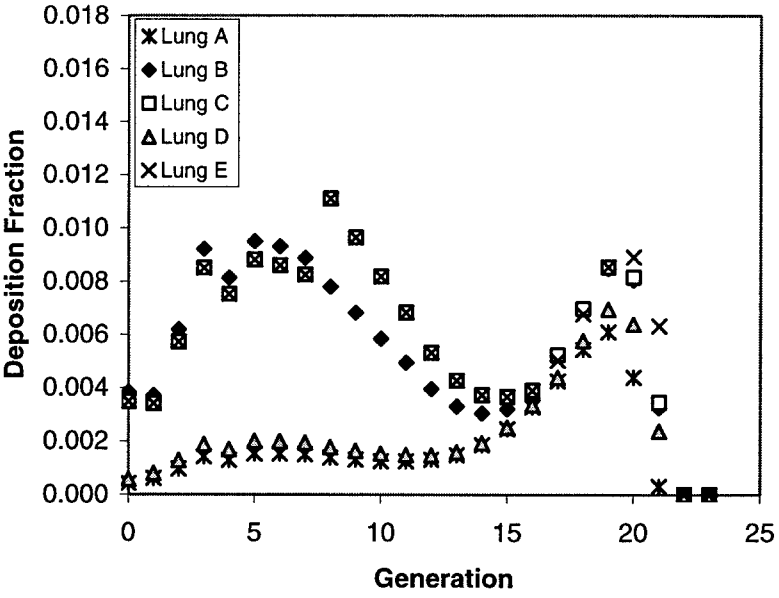

FIGURE 2. Effects of airway morphology changes on particle deposition fractions in the COPD lung model. Lung A, normal lung; Lung B, uniform airway reduction; Lung C, nonuniform airway reduction; Lung D, alveolar degeneration; Lung E, nonuniform airway reduction and alveolar degeneration.

particular change in the diseased lung morphology. The curve labeled Lung A represents deposition in a healthy lung (control case) that has been scaled based on the FRC value (corresponding to lung morphology A in the Methods). The curve labeled Lung B represents uniform constriction of the airways in generations 0–16 (lung morphology B). The curve labeled Lung

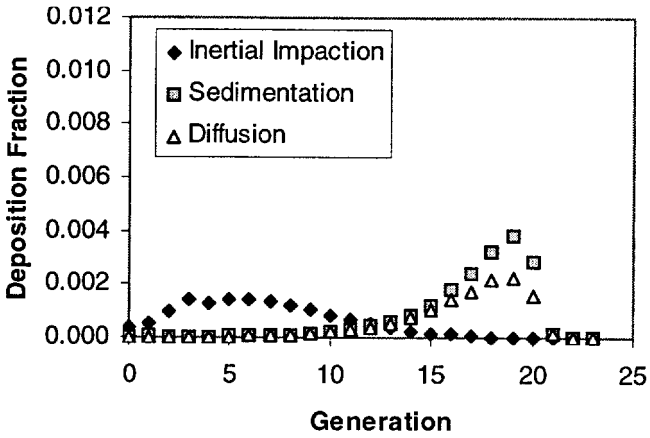

FIGURE 3. Deposition fraction as a function of airway generation for the three identified deposition mechanisms. Lung morphology A (normal lung) was used to account for subject variability based on the patients' FRC values.

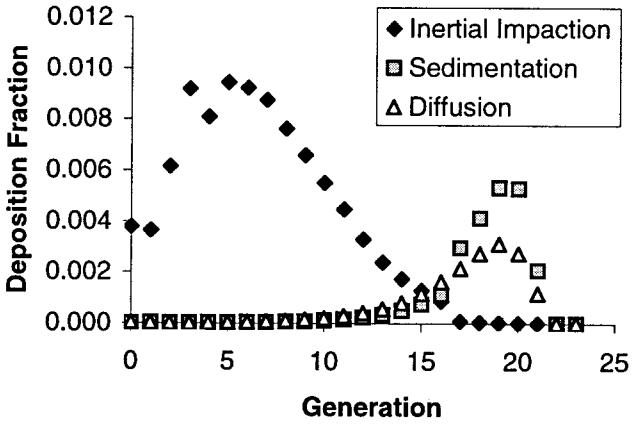

FIGURE 4. Deposition fraction as a function of airway generation for the three identified deposition mechanisms. Parabolic flow profile was used for calculation. COPD was modeled by lung morphology B (uniform reduction of the airway diameters in generations 0–16).

C represents nonuniform constriction of the airways in generations 0–16 (i.e., 0–7 have been constricted less than 8–16) (lung morphology C). The curve labeled Lung D represents deposition when the alveolar volume has been increased by 30% but no modification has been made in generations 0–16 (lung morphology D). The curve labeled Lung E represents deposition where the alveolar volume was increased by 30% and then a nonuniform constriction was imposed on the airways in generations 0–16 (lung morphology E). Clearly, airway constriction representing the effects of chronic bronchitis has the greater effect on the deposition fraction of inhaled PM (compare the curves Lungs B, C, and E to Lungs A and D).

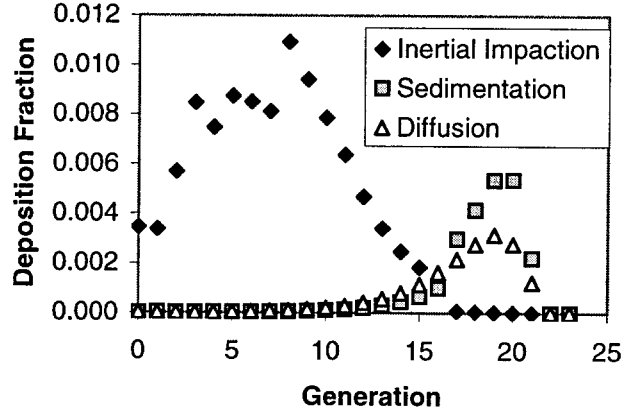

FIGURE 5. Deposition fraction as a function of airway generation for the three identified deposition mechanisms. COPD was modeled by lung morphology C (nonuniform reduction of the airway diameters in generations 0–16).

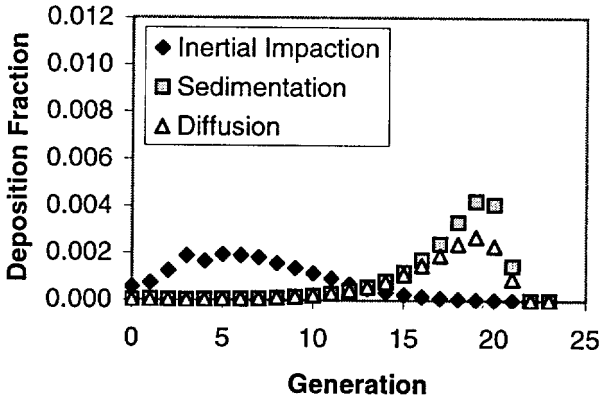

FIGURE 6. Deposition fraction as a function of airway generation for the three identified deposition mechanisms. COPD was modeled by lung morphology D (increased alveolar volumes).

Figures 3–7 show the breakdown of deposition by three mechanisms for the various morphological changes already identified for lung morphologies A, B, C, D, and E, respectively. If the separate curves in one of these figures were considered using the Superposition Principle, one of the corresponding curves from Figure 2 would result (e.g., superimposing the curves in Figure 3 would give the curve labeled Lung A in Figure 2). When there is no constriction of the airways (Figure 3), diffusion is the dominant mechanism of deposition, and the particles are primarily deposited in the pulmonary region. When the airways in generations 0–16 are narrowed (Figure 4), deposition by inertial impaction is markedly enhanced in the TB region (compare Figures 3 and 4). We also observe a very small increase in deposition by diffusion and sedimentation in the pulmonary region. When the constriction is

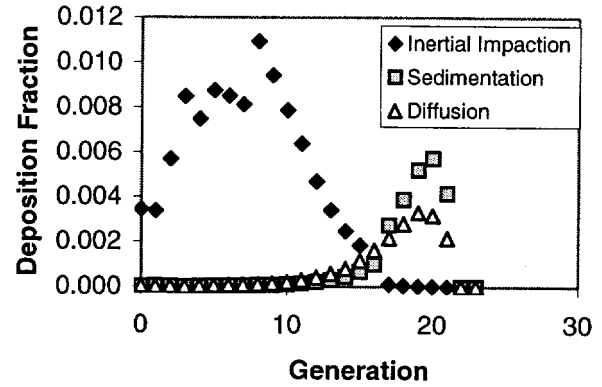

FIGURE 7. Deposition fraction as a function of airway generation for the three identified deposition mechanisms. COPD was modeled by lung morphology E (nonuniform reduction of the airway diameters in generations 0–16 and increased alveolar volumes).

nonuniform (Figure 5) we see a further, but slight, increase in deposition by inertial impaction (compare Figures 4 and 5). There is a noticeable change in the shape of the inertial impaction efficiency curve. At generation 6, airway constriction increases, and there is a large jump in the amount of deposition. If the alveolar volumes are increased (Figure 6), there is a slight decrease in deposition by diffusion and sedimentation in the pulmonary region (compare Figures 3 and 6). There is no change in deposition totals due to sedimentation and diffusion when we increase alveolar volumes as well as incorporate nonuniform constriction of the TB region (Figure 7) because the increase in deposition due to airway narrowing is balanced by the decrease due to emphysema.

From these systematic comparisons of Figures 3–7, it is apparent that the reduction in airspace within the TB region has the largest single effect on the total deposition of inhaled PM. When the model lung is scaled to have the same Raw value as the individual human subject considered (as in Figures 4, 5, and 7), there is a large decrease in the diameters of the airways. Because the airways in the TB region have been narrowed, the inhaled air travels with a higher velocity than it would in the non-COPD lung (Figure 3). This is important to note because it increases particle deposition by inertial impaction which is proportional to the magnitude of the velocity. We also see that the deposition in generations 17–23 is slightly higher when the alveolar volumes are not modified (Figures 4 and 5). This is due to an increase in deposition by sedimentation and diffusion. Because the velocities in the TB region are higher, the time to traverse the TB airways is decreased and, since the inhalation time is fixed at 1 s, the residence time in the pulmonary region is longer. Deposition efficiencies for the mechanisms of sedimentation and diffusion depend directly on residence time, hence we observe higher deposition in generations 17–23 in the COPD lung. Alternatively, we could base the analysis on the difference in airway volume in COPD lung versus the non-COPD lung. Because the volume of the TB region is reduced the inhaled aerosol mass will penetrate deeper into the pulmonary region in a COPD lung, thus allowing for greater deposition by mechanisms that are residence time dependent (i.e., sedimentation and diffusion). On the other hand, an increase in alveolar volume due to emphysema results in a slight decrease in deposition because particles need to travel a longer distance to deposit on the airway wall.

CONCLUSIONS

Patients with airway diseases (e.g., COPD) have been identified as critical subpopulations to be addressed in health risk assessment for air pollutants. To understand why these patients are more susceptible to inhaled PM, it is first necessary to study dosimetry as affected by COPD. This article has presented a viable, deterministic model for particle deposition in COPD lungs. The core PM deposition model has been validated by comparisons

of theoretical predictions with data from healthy (i.e., control) test subjects. The format of the model was specifically designed to permit the disease-induced effects of COPD on airway morphologies to be described by inclusions of:

- Chronic bronchitis (narrowing of TB airway diameters).
- Emphysema (deterioration of alveolar walls).
- Combinations of these two effects.

An additional benefit of using the model was that we were able to investigate the respective roles of different deposition mechanisms. The main conclusions are:

- Chronic bronchitis is the main cause of increased PM deposition in COPD patients, relative to emphysema.
- The increase in PM deposition takes place primarily in the TB region as a result of increased efficacy of the inertial impaction mechanism.

REFERENCES

Anderson, P. J., Blanchard, J. D., Brain, J. D., Feldman, H. A., McNamara, J. J., and Heyder, J. 1989. Effects of cystic fibrosis on inhaled aerosol boluses. *Am. Rev. Respir. Dis.* 140:1317–1324.

Bennett, W. D., Zeman, K. L., Kim, C., and Mascarella, J. 1997. Enhanced deposition of fine particles in COPD patients spontaneous breathing at rest. *Inhal. Toxicol.* 9:1–14.

Hughes, J. M. B., Hoppin, F. G., and Mead, J. 1972. Effect of lung inflation on bronchial length and diameter in excised lungs. *J. Appl. Physiol.* 32(1):25–35.

Hyatt, R. E., and Wilcox, R. E. 1961. Extrathoracic airway resistance in man. *J. Appl. Physiol.* 16:326–330.

Kim, C. S. 1989. Aerosol deposition in the lung with obstructed airways. *J. Aerosol Med.* 2:111–120.

Kim, C. S., and Eldridge, M. A. 1985. Aerosol deposition in the airway model with excessive mucus secretions. *J. Appl. Physiol.* 59:1766–1772.

Kim, C. S., and Kang, T. C. 1997. Comparative measurement of lung deposition of inhaled fine particles in normal subjects and patients with obstructive airway disease. *Am. J. Respir. Crit. Care Med.* 155:899–905.

Kim, C. S., Brown, L. K., Lewards, G. G., and Sackner, M. A. 1983. Deposition of aerosol particles and flow resistance in mathematical and experimental airway models. *Appl. Physiol. Respir. Environ. Exercise Physiol.* 55(1):154–163.

Kim, C. S., Lewars, G. A., and Sackner, M. A. 1988. Measurement of total lung aerosol deposition as an index of lung abnormality. *J. Appl. Physiol.* 64:1527–1536.

Kim, C. S., Abraham, W. M., Chapman, G. A., and Sackner, M. A. 1989. Enhanced aerosol deposition in the lung with mild airways obstruction. *Am. Rev. Respir. Dis.* 139:422–426.

Kuempel, E. D., Tran, C. L., Bailer, A. J., Smith, R. J., Dankovic, D. A., and Stayner, L. T. 2001. Methodological issues of using observational human data in lung dosimetry models for particulates. *Sci. Total Environ.* 274:67–77.

Laube, B. L., Swift, D. L., Wagner, H. N., Jr., Norman, P. S., and Adams, G. K. III. 1986. The effect of bronchial obstruction on central airway deposition of a saline aerosol in patients with asthma. *Am. Rev. Respir. Dis.* 133:740–743.

Lazaridis, M., Broday, D. M., Hov, O., and Georgopoulos, P. G. 2001. Integrated exposure and dose modeling and analysis system: Deposition of inhaled particles in the human respiratory tract. *Environ. Sci. Technol.* 35:3727–3734.

Martonen, T. B. 1982. Analytical model of hydroscopic particle behavior in human airways. *Bull. Math. Biol.* 44(3):425–442.

Martonen, T. B. 1993. Mathematical model for the selective deposition of inhaled pharmaceuticals. *J. Pharm. Sci.* 82(12):1191–1199.

Martonen, T. B., and Katz, I. M. 1993a. Deposition patterns of aerosolized drugs within human lungs: Effects of ventilatory parameters. *Pharm. Res.* 10(6):871–878.

Martonen, T. B., and Katz, I. M. 1993b. Deposition patterns of polydisperse aerosols within human lungs. *J. Aerosol Med.* 6(4):251–274.

Martonen, T. B., and Katz, I. M. 1994. Inter-related effects of morphology and ventilation on drug deposition patterns. *S.T.P. Pharma Sci.* 1:11–18.

Martonen, T., Zhang, Z., and Yang, Y. 1995. Interspecies modeling of inhaled gases. *Inhal. Toxicol.* 7:1125–1139.

National Lung Health Education Program. 1998. Strategies in preserving lung health and preventing COPD and associated diseases. *Chest* 113(2 supplement):123S–163S.

Pedley, T. J., Schroter, R. C., and Sudlow, M. F. 1970. The prediction of pressure drop and variation of resistance in the human bronchial airways. *Respir. Physiol.* 9:387–405.

Rennard, S. I. 1998. COPD: Overview of definition, epidemiology and factors influencing its development. *Chest* 113(suppl. 4S):235S–241S.

Schwartz, J. 1996. Air pollution and hospital admissions for respiratory disease. *Epidemiology* 7:20–28.

Seaton, A., MacNee, W., Donaldson, K., and Godden, D. 1995. Particulate air pollution and acute health effects. *Lancet* 345:176–178.

Segal, R. A., Martonen, T. B., and Kim, C. S. 2000. Comparison of computer simulations of total lung deposition to human subject data in healthy subjects. *J. Air Waste Manage. Assoc.* 50:1262–1268.

Smith, S., Cheng, U. S., and Yeh, H. C. 2001. Deposition of ultrafine particles in the human tracheobronchial airways of adults and children. *Aerosol Sci. Technol.* 35:697–709.

Svartengren, M., Anderson, M., Bylin, G., Philipson, K., and Camner, P. 1990. Regional deposition of 3.5 μm particles in subjects with mild to moderately severe asthma. *J. Aerosol Med.* 3:197–207.

Weibel, E. R. 1963. *Morphometry of the human lung.* New York: Academic Press.

Wordley, J., Walters, S., and Ayres, J. G. 1997. Short term variation in hospital admissions and mortality and particulate air pollution. *Occup. Environ. Med.* 54:108–116.